MXenes: Two-Dimensional Futuristic Material

Uday Karanbir Singh[1]*, Harpreet Kaur[1], Taranveer Kaur[1], Pushpinder Kaur[2], Richa Rastogi[1]*

[1]Centre for Nanoscience & Nanotechnology, Panjab University, Chandigarh.

[2]Department of Chemistry, Sri Guru Gobind Singh College, Sector-26, Chandigarh

Corresponding author E-mail id: sainiuday1@gmail.com, richa.bend@gmail.com

1. INTRODUCTION

Two-dimensional (2D) layered materials are a rapidly expanding group of nanostructured materials with distinctive physiochemical properties. These nanomaterials have been used in a diverse range of applications in recent years [1]. 2D materials are specifically characterized by one dimension being restricted to a few nanometers (less than 5 nm), while the other dimensions can reach up to 100 nm or a few micrometers [1] – [3].

A notable addition to this category is MXenes, which have gathered significant attention since their discovery [4]. MXenes belong to a new group of transition metal nitrides, carbides, or carbonitrides, flaunting unique morphological structures and exceptional properties applicable to different fields similar to gas sensing, electromagnetic hindrance (EMI) shielding, energy storage, and membrane-grounded water filtration [5]. These MXenes are typically produced through the delamination of three-dimensional (3D) ternary or quaternary compounds chemically; that are known as MAX phases. The formula $M_{n+1}AX_n$ (n = 1, 2, or 3) represents MAX phases; where M represents a transition metal such as Cr, Zn, Ti, Mo, etc. and A represents elements from groups 13 and 14 in the periodic table while X denotes carbon (C) and/or nitrogen (N), and [6].

MAX phases are technologically significant materials due to their intriguing combination of ceramic and metallic characteristics [7].

MXenes are typically produced by a chemical etching process selectively that detaches layers of A elements from their precursor MAX-phases. Till now, more than 30 structurally different MXenes have been synthesized successfully whereas many others have been theoretically predicted [8]. $M_{n+1}X_nT_n$ or $M_{1.33}XT_n$ represents the general formula for MXenes. Here, M represents a transition metal, X represents either C and/or N, and T represents the surface terminal group like O, F, or OH [9]. Depending on the value of n in MAX phases, the resulting MXenes can have M_3X_2, M_2X, or M_4X_3 lattice structures [10], as shown in Fig.1. MXenes possess a layered structure where MX layers are stacked with the single surface group terminations. The stacking types of MX layers, namely Bernal stacks or simple hexagonal (SH) are determined by the relative position of the layers with terminations. Surface groups are connected to these layers through dihydrogen bonding, while the intralayer are held together by strong ionic and covalent bonds.

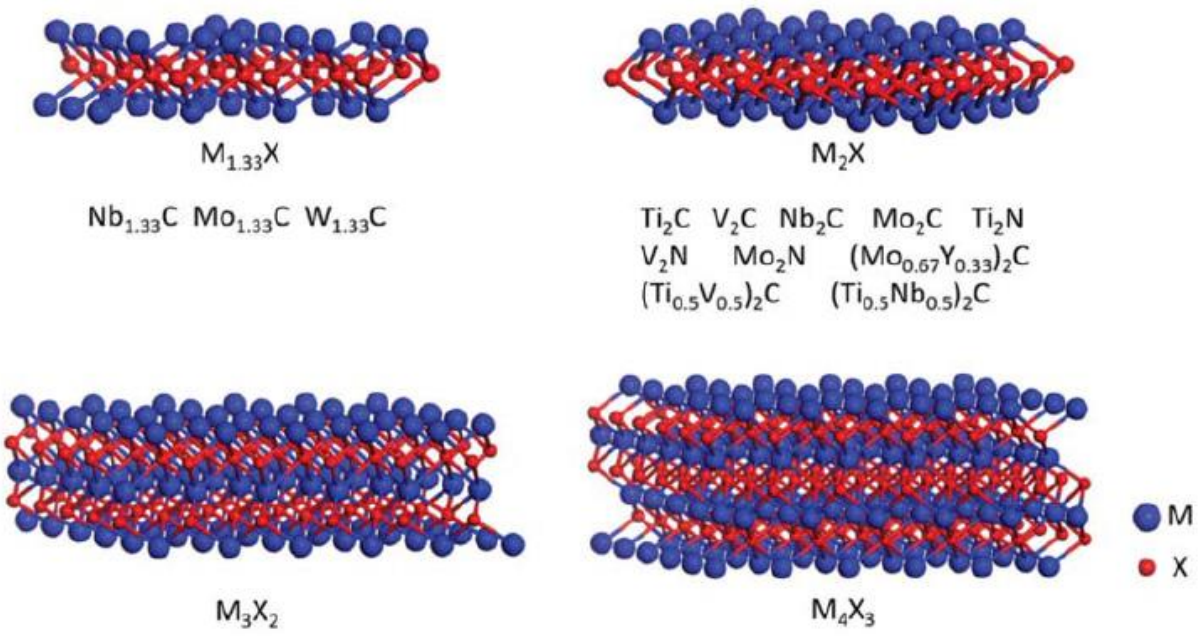

Fig 1. Illustration of schematics depicting an overview of experimentally synthesized MXenes. Reprinted with authorization from ref. [110], copyright 2020, Nanophotonics.

MXenes are characterized by numerous M elements and two kinds of structures viz. ordered phases and solid solutions (Fig.2). Solid solutions refer to the random arrangement of two similar or different transition metals in M layers, while ordered phases involve a single or double layers of a transition metal in which the first transition metal layer is intercalated between the layers of the second metal in the 2D carbide structure [11]. The properties of MXenes, including their electronic and optical characteristics, are closely linked to M elements and T surface functional groups. The combination of features exhibited by MXenes is remarkable, such as high surface area, excellent flexibility, 2D surface morphology, hydrophilicity, metallic conductivity, and mechanical strength [12]. The metal-like conductivity arises here due to the presence of free electrons in transition metal carbides or nitrides, while the hydrophilicity is a result of the surface terminations. The different transition metals, along with different surface functional groups, enable tuning of MXene properties. Consequently, MXenes possess versatile and diverse surface chemistry, making them suitable for enormous applications in various fields of research.

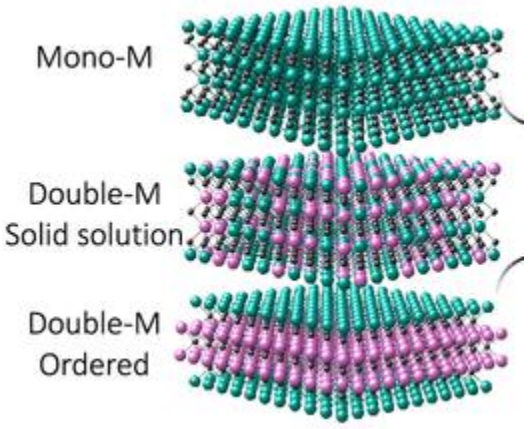

Fig 2. Types of MXenes structures : mono-M elements (For instance, Ti_2C); Double- M solid solution where at least two different M elements (for instance, $(Ti,V)_3C_2$; ordered double-M solid solutions containing one transition metal in perimeter layers and another in the center (for instance, Mo_2TiC_2, in which outer M layer are made up of Mo and center M layer is Ti). Reprinted from authorization from ref.[111] , copyright 2021, ACS nano.

2. STRUCTURE AND PROPERTIES OF MXENES

2.1. Structure of MXene: -

The synthesis of MXenes primarily involves wet etching of MAX phases. In MAX phases, the metallic M atoms are arranged in a hexagonal close-packed (hcp) structure, where X atoms occupy the octahedral interstices. These interstices are interleaved between the layers of group A elements in the $P6_3/mmc$ space group [13]. Once the A layers are removed, the remaining $M_{n+1}X_n$ layers form a 2D hexagonal close-packed structure, with the addition of F, O, H, OH, and/or Cl atoms. Functional sites of MXenes are always fully occupied, as evidenced by the negative values of formation energy when surface endings bond with the outer layers of transition metals [14]. Fully terminated MXenes also possess positive phonon frequencies [15] Different configurations are possible for functional group terminations in MXenes. Three common types are considered (Fig. 3a): Type I, where functional groups are placed above the unfilled sites of three neighboring X atoms and direction towards the M atoms in the second atomic layer of Ti; Type II, where functional groups are positioned over the topmost sides of the X atoms; and Type III, which is in between of Types I and II, with one functional group above the unfilled sites of the X atoms and another functional group over the top sites of the X atoms on the other sides. Theoretical calculations have proved that Type I configuration is the most stable for the majority of MXenes [13] – [15].

The conductivity of MXenes is influenced by the anisotropy resulting from weak interlayer bonding which is almost 2 to 6 times larger than that of well-known 2D materials like graphite and MoS_2 and the strong intralayer bonding. The interlayer coupling needs to be weakened for successful exfoliation into monolayers, but their layered structure is stable due to the relatively stronger interlayer bonding

Functional groups play crucial roles in MXenes' applications, such as energy storage. However, the experimental results do not agree with the theoretical predictions because of the simplified models used in theoretical studies. The functionalization reactions of MX layers involve a competitive and spontaneous adsorption process, resulting in a coexisting feature of terminations that maximizes entropy. Among the functional groups, -O terminations are more stable due to their stronger covalent bonding with the transition metal of the MX layer [16].

As depicted in Fig 3(c), The MXene etched by Hydrogen Flouride (HF) exhibits a layered structure with the value of "*c"* lattice parameter as 19.8 Å [17], and a non-uniform interlayer spacing is observed in the high-angle annular dark-field scanning transmission electron microscopy (HAADF-STEM) images. The interlayer interactions between different terminations lead to inhomogeneous interlayer spacing and imply the coexistence of functional groups. The homogeneity of layered domains can be improved with annealing in ammonia or intercalation of cations. STEM images and XRD patterns confirm the changes in interlayer spacing and crystallinity after intercalation or annealing.

MXenes are not structurally perfect and exhibit point defects, such as Ti vacancies caused by the etching process. The concentration of etchant can control the concentration of vacancies [18]. Point defects, including vacancies and adatoms, offer opportunities to modulate the surface properties of MXenes that are important for catalytic and energy storage applications.

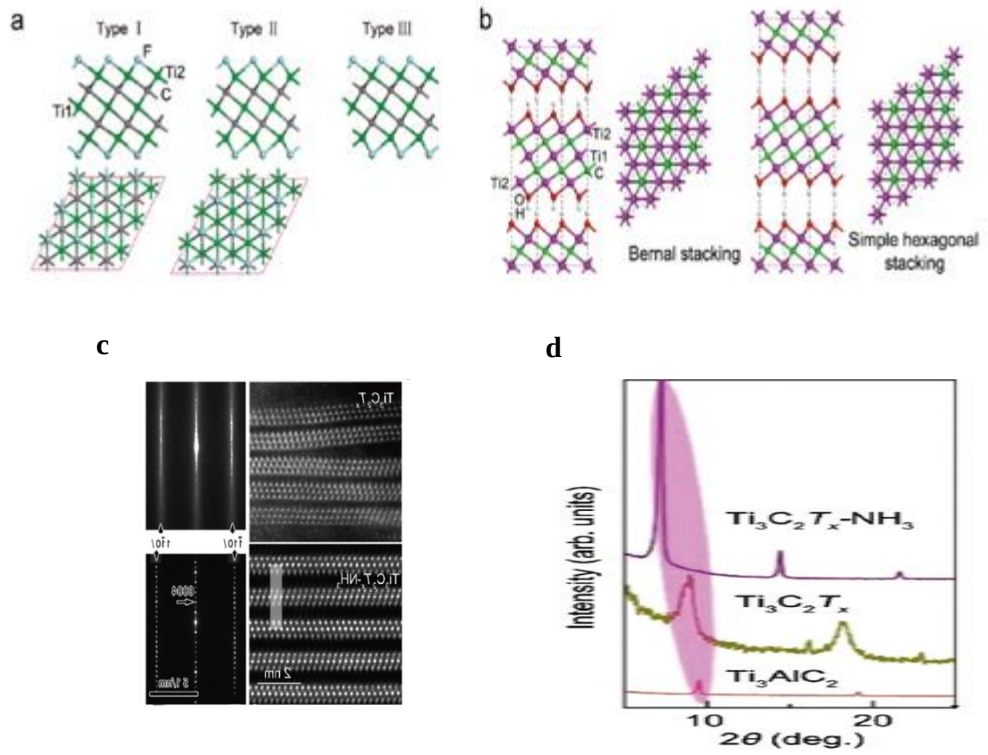

Fig 3 (a) Fig 3 illustrates several $Ti_3C_2F_2$ structural topologies with various orientations of surface F atoms from top and side perspectives. (source: American Chemical Society, copyright 2012, ref. [112]). (b) Fig. 3 also presents projections of two distinct layering types of $Ti_3C_2(OH)_2$ shown here (source: Nature, copyright 2015, ref. [113]). (c) The structure and diffraction patterns of $Ti_3C_2T_x$ and annealed $Ti_3C_2T_x$ in ammonia are captured through STEM imaging along the [11 %20] zone axis (source: American Chemical Society, copyright 2014, ref. [114]; copyright 2019, ref. [115]; and copyright 2019, ref. [116]). (d) Displayed are the X-ray diffraction (XRD) patterns of annealed $Ti_3C_2T_x$, Ti_3AlC_2, and $Ti_3C_2T_x$ in ammonia. (source: American Chemical Society, copyright 2019, ref. [116]).

Characterization techniques like scanning transmission electron microscopy (STEM) with annular dark-field imaging enable the identification of MX layer structures, while other methods like Raman spectroscopy and NMR studies provide indirect information about the composition and distribution of functional groups. MXene layers can be identified through significant shifts observed in the (00l) plane reflections in the patterns of XRD when MXene powders get dried [19]. However, MXenes without terminations, except for TaC, WC, and Mo_2C crystals synthesized through CVD, have not been successfully produced yet [20]. Moreover, the

preparation of MXenes with a mono-surface group functionalization is extremely challenging, and there are limited reports on this subject matter.

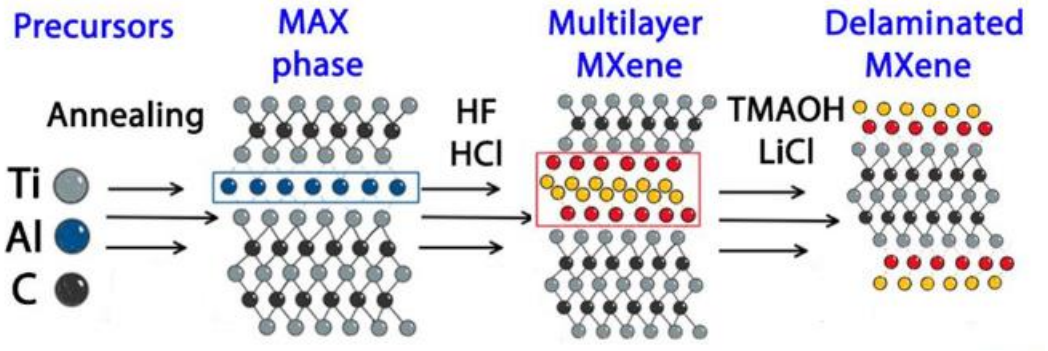

Fig 4. Demonstrating how MAX phase and MXene differ. Reprinted from authorization from ref. [117], copyright 2021, ACS Chemical Health and Safety.

2.2.Electrical and optical properties: -

The investigation of MXenes' electronic properties is driven by their significant application in electronic energy devices like electrochemical capacitors, sensors, etc. Bare MXenes exhibit metallic conductivity, as observed in their precursor MAX phases. However, when MXenes are functionalized with surface functional groups, their conductivity can be altered. For example, Ti_2C in its bare form shows metallic characteristics, but O-terminated MXenes like Ti_2CO_2 acquire semiconducting characteristics as the d band is shifted over the Fermi level. The type of termination also influences conductivity. MXenes functionalized with F, such as Ti_2CF_2, remain metallic in nature with their Fermi energy level located at the Ti layer's d band. Additionally, the M element also changes the electronic properties. Transitioning from $Ti_3C_2O_2$ to $Mo_2TiC_2O_2$ transforms metallic conductivity into a semiconducting nature [21]. Some of these semiconducting MXenes are Zr_2CO_2, Hf_2CO_2, and Sc_2CT_2 (T = O, F, OH). While certain MXenes, such as oxide $M'_2M''C_2$ (M' = Mo, W; M'' = Ti, Zr, Hf), are behave like an insulator [22]. MXenes defects like carbon vacancies in Ti_2CT_2, enhance their electronic conductivity [23].

In practice, MXenes synthesized by MAX phases are typically functionalized with diverse functional groups. Therefore, experimental assessments are necessary to

determine the properties of MXenes. Various MXene species, including Ti_2CT_x [24], $Ti_3C_2T_x$ [25], $TiNbCT_x$ [26], Ti_3CNT_x [26], $Ta_4C_3T_x$ [26], Mo_2CT_x [27], $Mo_2TiC_2T_x$ [28], and $Mo_2Ti_2C_3T_x$ [28], have been experimentally measured for their electronic properties. $Ti_3C_2T_x$, which is the first synthesized MXene, is the most conductive till now with its metallic nature indicated by a linear I-V curve [26]. This metallic $Ti_3C_2T_x$ exhibits potential as a supercapacitor electrode material. MXenes containing Mo exhibit semiconducting electrical behavior, that is more suitable for applications like transistors. However, 2D $Mo_{4/3}C$ sheets that possess ordered metal divacancies have high electrical conductivities, making them ideal for supercapacitor electrode materials [29]. The electrical conductivity behavior of MXenes is also influenced by the sample state and preparation method. $Ti_3C_2T_x$ flakes, vacuum-filtered [30] or spin-cast [31] films, demonstrate high electrical conductivity. The conductivity of multilayered MXenes shows anisotropy, with lower conductivity along the c-axis compared to the basal plane [32]. Intercalation and surface termination have been experimentally shown to impact MXene electronic properties. Vacuum annealing significantly reduces the resistance of multilayered MXenes by re-intercalation and partial removal of surface functional groups [33]. Surface group tuning also modifies carrier transport properties.

Furthermore, thinner $Ti_3C_2T_x$ MXene films are both transparent and conductive, which ensures their promising candidature for transparent conductive electrodes. For instance, a 5 nm-thick $Ti_3C_2T_x$ film has been investigated for its optical properties as a transparent conductive electrode that transmits 91.2% of visible light and has a resistance of 8 $k\Omega\ sq^{-1}$ [34], [35]. The optoelectronic behavior of these films can be tuned through cation intercalation. Therefore, when metallic MXenes are used as electrode material in supercapacitor applications, the preparation method should be carefully employed.

2.3.Mechanical properties: -

The electrochemical performance of electrode materials can be influenced by their mechanical properties, especially in flexible applications where they undergo pressure, bending, and twisting. The mechanical characteristics of MXenes have been investigated through theoretical calculations by considering parameters such as surface functionalities, composition, and thickness of the layer. Parameters such as out-of-plane rigidity (D) and in-plane stiffness (C) etc. play an important role in determining their elasticity and flexibility. The Foppl-von Karman numbers per area (C/D) of MXenes, which serve as flexibility descriptors, are comparable to those of the MoS_2 monolayer [36], indicating that MXenes are strong yet flexible materials. Reported in-plane Young's moduli of a bare monolayer of Ti_2C, Ti_3C_2, and Ti_4C_3 are 597 GPa, 502 GPa, and 534 GPa, respectively, which shows their lower strength than atomically thin graphene but higher strength than materials like MoS_2 and other 2D nanomaterials [37]. The calculated breaking strength of some bare MXenes structures (M = Sc, Mo, Ti, Zr, Hf; X = C, N; n = 1) ranges from 92 to 161 N m^{-1} [38], indicating good mechanical stability. Surface termination in $Ti_{n+1}C_n$ (n = 1, 2, and/or 3) MXenes can slow down the strength collapse of surface atomic layers and enhance their mechanical flexibility [39], which enables them to sustain high strains under tensile loading.

Experimental investigations have also been done to examine the mechanical properties of MXenes. Nanoindentation experiments on individual layers of $Ti_3C_2T_x$ demonstrated Young's modulus of approximately 0.33 TPa [40]. It is the highest demonstrated value among solution-processed 2D materials, including graphene oxide. $Ti_3C_2T_x$ films exhibit remarkable mechanical robustness and flexibility, as a 5 mm-thick film can withstand about 4000 times of its weight (approximately 1.3 MPa) without any visible deformation or damage observed and can be easily folded [41]. The mechanical properties of $Ti_3C_2T_x$ films can be further improved by making composites with artificial or natural polymers [41] such as cellulose [42] nanofibrils. Additionally, during the period of an electrochemical reaction involving alkaline cation intercalation/extraction, the elastic modulus that is normal to the electrode

surface undergoes reversible changes, ensuring structural stability during prolonged charge/discharge cycles [43].

2.4. Chemical stability: -

Based on a study of Bader charge, M elements' oxidation number in MXenes is significantly less than that of their associated oxides, which are the species that have the most thermodynamical stability [44]. This suggests that MXenes are prone to oxidation. Interestingly, MXenes' oxidation status is highly altered via the functional terminations and is adjustable by mild oxidation, where noble metal ions serve as oxidants and MXenes serve as reductants. Mild oxidation, as opposed to total oxidation, permits structural integrity preservation while promoting the production of noble metal nanoparticles. Notably, these nanoparticles of noble metal are equally dispersed on MXenes, giving them appealing surface-enhanced Raman scattering properties [45].

In the fabrication of films or coating electrodes, Water-based colloidal solutions of delaminated MXene flakes have been widely employed. As a result, the stability of MXene suspensions is vital to the investigation. $Ti_3C_2T_x$ MXene solutions in ambient environments degrade completely within 15 days, primarily forming anatase TiO_2 because the major oxidant for MXene flakes is dissolved oxygen [46]. As an antioxidant, sodium L-ascorbate can be used to keep colloidal $Ti_3C_2T_x$ MXene from oxidizing [47]. The quality guarantee period increases significantly when the $Ti_3C_2T_x$ MXene is dried. However, the conductivity of MXene flakes degrades over time due to edge oxidation. Furthermore, re-dispersing the dried sample in water becomes challenging. The degrading process is also affected by MXene size, with smaller flakes being less stable and multilayered MXene exhibiting greater stability than monolayered MXene. Additionally, light exposure hastens the oxidation process [48]. MXene should be kept in a hermetically sealed container filled with argon at a temperature of 5°C in a dark environment to extend its storage time.

In terms of thermal stability, dried MXenes show varying levels of oxidation resistance behaviors based on their composition and the immediate surroundings. Multilayered Ti_2CT_x converts into TiO_2 nanocrystals on thin graphitic nanosheets in air at 227°C [49]. $Ti_3C_2T_x$ undergoes the partial transformation at 200°C into anatase (TiO_2) and completely oxidizes at 1000°C into rutile (TiO_2), releasing H_2O and CO_2 in an oxygen-rich atmosphere, although its stability cannot match that of graphite. $Ti_3C_2T_x$ is stable in an argon environment and remains stable up to temperatures of 800°C [50]. In the case of Nb_2CT_x, the surfaces are heavily adorned with Nb adatoms that draw and associate with ambient oxygen species, creating clusters that expand over time. Below 375°C, V_2CT_x MXene remains stable in an argon environment at temperatures but begins to degrade at 150°C in an air atmosphere [51], [52].

3. SYNTHESIS OF $Ti_3C_2T_X$ MXENE

The exceptional parts of $Ti_3C_2T_x$ are related to its conflation processes, which determine its electrical conductivity, chemical composition, etching effectiveness, side size, blights, and face terminations. Since the original conflation of $Ti_3C_2T_x$ in 2011, experimenters have conducted expansive examinations into the new MAX phase and the drawing system. Fluoride-grounded swab drawings, fluoride drawings, and fluoride-free drawings are some of the colorful etchants currently being investigated for the $Ti_3C_2T_x$ MXene product. The electrochemical performance of $Ti_3C_2T_x$ MXene is significantly influenced by these various drawing techniques.

3.1. HF Etching: -

The A layer of the MAX phase is commonly etched to prepare MXene, and the method is as follows [53], [54]:

$$M_{(n+1)}AX_n + 3HF = AlF_3 + 1.5H_2 + M_{(n+1)}X_n \quad \text{.....(1)}$$

$$M_{(n+1)}X_n + 2H_2O = M_{(n+1)}X_n(OH)_2 + H_2 \quad \text{.....(2)}$$

$$M_{(n+1)}X_n + 2HF = M_{(n+1)}X_nF_2 + H_2 \quad \text{.....(3)}$$

In reaction (1), the $M_{n+1}X_n$ phase is created as a result of the A components being removed from the MAX phase. Functional groups like -F and/or -OH are produced as a result of reactions (2) and (3). The structural morphology of Ti_3AlC_2 is characterized in Figure 5 along with the exfoliation process. $Ti_3C_2T_x$ MXene with an accordion-like form was synthesized by Naguib et al. by etching Ti_3AlC_2 powders for two hours in a 50% concentrated HF solution. [55]. Using a 50% HF solution, Mashtalir et al. [56] investigated the impact of process variables and particle size on the etching process of Al from Ti_3AlC_2. The results showed that decreasing bulky Ti_3AlC_2's starting particle size, extending the reaction time, and raising the immersion temperature promoted the transformation of $Ti_3C_2T_x$. [57]. The etching procedure is significantly influenced by the duration of etching, temperature, and HF concentration. Up to 5% of HF may be used to successfully remove Al from the Ti_3AlC_2 MAX phase. However, when HF attention surpasses 10%, a flyspeck morphology resembling an accordion is typically seen. Additionally, when HF concentration rises, flaws in the $Ti_3C_2T_x$ flakes become more prevalent, which affects the final MXene's quality, environmental stability, and other characteristics. [58], [59]. Despite the fact that the HF technique is simple to use and has a low reaction temperature, it should be noted that the HF etchant is extremely corrosive, and poisonous, poses operational dangers, and has negative environmental impacts..

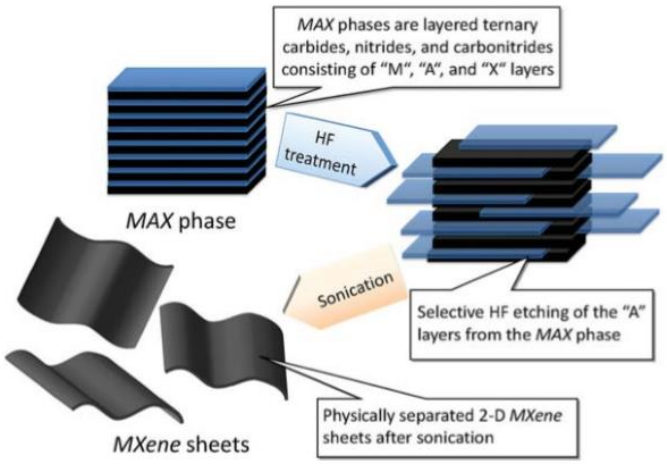

Fig 5. An example of a schematic showing how to create MXene utilizing HF as an etchant to produce single-layered MXene configuration from the MAX phase. Reproduced from ref. [118], copyright 2012, America Chemical Society, with permission.

3.2. Acid/fluoride salt or Hydrofluoride Etching: -

In addition to HF etching, gentler fluorine-containing etchants including HCl/KF, HCl/NH_4F, HCl/NaF, $(NH_4)HF_2$, HCl/LiF, and HCl/FeF_3, have been created for the in-situ HF etching manufacturing. It is crucial to remember that these etchants are only appropriate for creating Ti3C2Tx MXene and might not work for other MXenes. To produce very pure V2C MXene, for instance, only the NaF/HCl etchant is effective [60], although it needs a longer etching time than pure HF etching, it improves the safety of the experimental procedure. These etchants still produce MXene with an accordion-like layering morphology [60]. Cations like Na^+, Fe^{3+}, $NH4^+$and K^+ are concurrently intercalated into the MXene interlayers during the etching process. Compared to pure MXene, the structure of the layers is more open and homogeneous as a result of the cation intercalation, and the atomic layers are spaced more uniformly. Fe^{3+} cations partly oxidize the surface Ti after etching Ti_3AlC_2 with HCl/FeF_3, as a result of the extraction of Al. [61].

Among the etchants discussed, HCl/LiF has been predominantly used and proven to be the most effective. Delamination is accomplished by using the proper concentration (7.5 M LiF in 9 M HCl) and the intercalation of solvated Li^+ ions. As a result, hand-shaking may easily produce bigger single- or few-layer MXene flakes with fewer flaws without the need for sonication or further intercalation. [62]. The precursor MAX phases chosen affect the sizes and forms of the resultant MXenes, allowing researchers to choose the best MAX phases based on their unique study goals. Notably, the intercalation of Li^+ ions causes changes in the rheological characteristics of the MXene sediment, which behaves like clay [63]. This offers new processing options such as direct film production through rolling. Furthermore, potential tests (-30 to -80 mV) show that the MXene sediment exhibits better hydrophilicity attributable to surface O-containing groups and a large negative surface charge [64]. As a result, the MXene can be easily dispersed in water and

processed using techniques like writing [67], spray coating [65], spin coating [64], and printing [66].

Compared to pure HF etching, the LiF/HCl etching method provides several advantages, even if it takes more time to etch. The surface termination of the MXene is affected by the synthesis process, according to NMR characterization. HF-etched MXene has over four times more -F termination than MXene that has been etched with LiF/HCl. However, it is known that -F groups have a detrimental effect on MXene's electrochemical performance, which explains why HF-etched MXene shows decreased capacitance. It's interesting to note that by acid etching, sputtering-deposited MAX thin films may be immediately transformed into MXene epitaxial thin films.

For the manufacture of MXene, HCl/LiF has shown to be a successful etchant, providing both exfoliation and delamination effects. However, it remains a puzzle as to why only HCl/LiF etchant exhibits these properties. Preliminary research by Lerf et al. 1977[68] indicates that the existence of bigger anion than F^- or O^{2-} during etching, such as Cl^-, Br^-, I^-, SO_4^{2-}, and PO_4^{3-}, results in more open MXene interlayers. These anions are thought to adsorb at the margins of MXenes, serving as supports to open the edges and making it simpler for water to enter the interlayer. An HCl solution is favored during etching because among these anions, Cl^- is easily adsorbed into MXene edges and exhibits a large synergistic impact on swelling [69].

Regarding cations, Li+ ions can enter the interlayer gap accompanied by water molecules, resulting in swelling and delamination [69]. Exploring the effects of various ions during etching is crucial to developing more effective and rational methods for MXene preparation.

3.3. Alkali Etching: -

According to our present knowledge, protons and fluoride ions are necessary for the production of MXene during acidic solution etching. However, considering the hazards associated with hydrofluoric acid (HF) and the negative impact of -F groups on MXene's electrochemical performance, alternative fluorine-free procedures are urgently needed. A lot of work has gone into creating fluorine-free alkali etching techniques.

One approach involves removing the Al layer from Ti_3AlC_2 using tetramethylammonium hydroxide (TMAOH) after briefly pretreating the surface with 20–30 wt% HF [70]. However, it has been shown that HF and TMAOH both contribute to the etching process because employing simply TMAOH as the etchant fails to provide the required results. Another method includes combining sonication and TBAOH (tetra-n-butylammonium hydroxide) intercalation to create smaller MXene structures like quantum dots [71].

Inorganic alkalies have also been used often in Ti_3AlC_2 etching in addition to organic alkalies. MXenes have been made using a hydrothermal process with inorganic alkali assistance. Successful $Ti_3C_2T_x$ powder synthesis has been achieved at increased temperatures of 270°C for NaOH aqueous solution and 180°C for KOH solution with a small quantity of water. With a purity of 92 weight percent, this inorganic alkali-based technique produced multilayer $Ti_3C_2T_x$ with -OH and -O terminations [72].

4. MXENE APPLICATIONS

MXenes, a groundbreaking class of two-dimensional nanosheets, have opened up a world of possibilities in various applications. With their remarkable conductivity and customizable properties, these materials are at the forefront of revolutionizing technologies such as supercapacitors with rapid charging capabilities and developing advanced drug delivery systems with unique properties to precisely target and release

therapeutic agents, leading to more effective treatments with reduced side effects. The uses of MXene in many domains are given below.

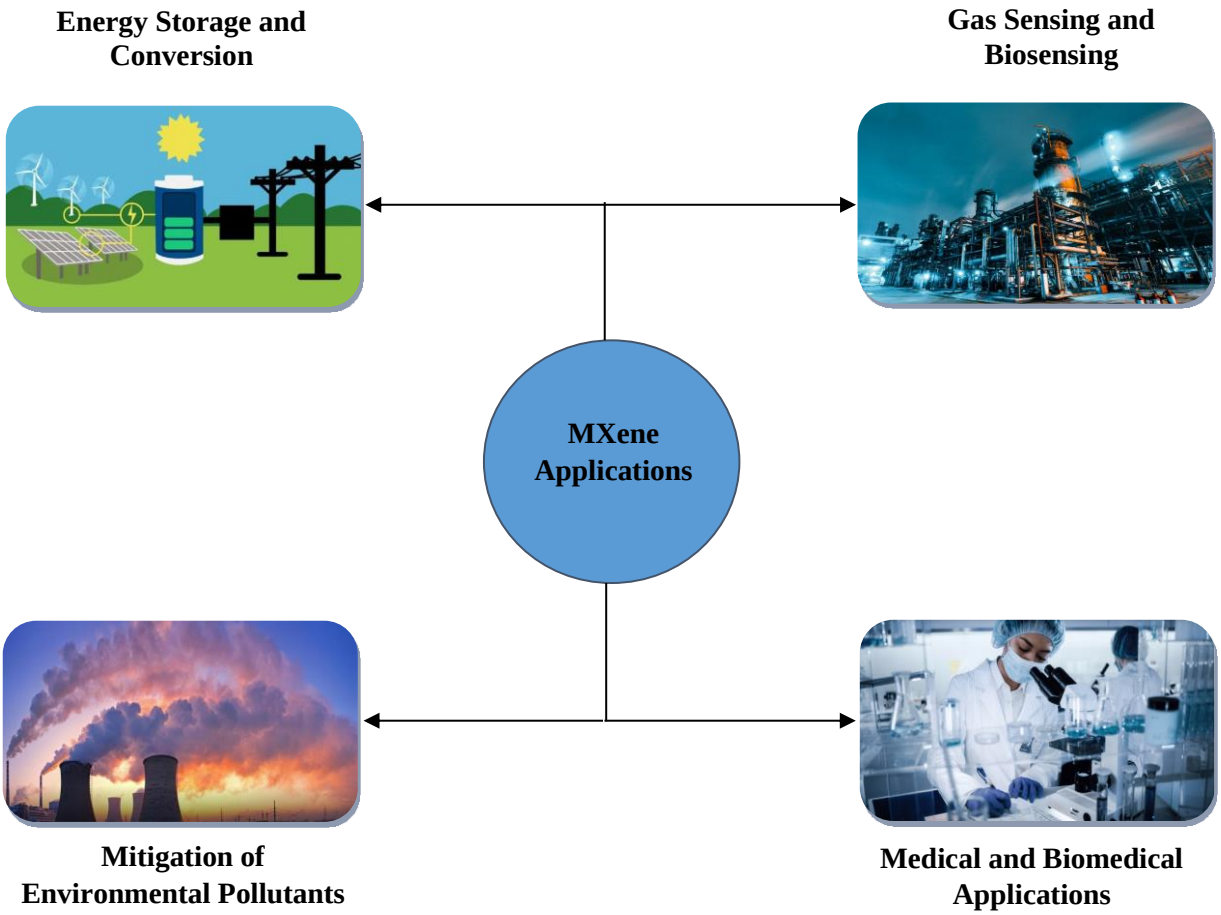

Fig 3. Showing applications of MXene in different fields.

4.1. Storage and conversion of energy: -

Due to their desirable characteristics, such as their high Young's modulus, outstanding electrical conductivity, and adaptable surface chemistry, MXenes are extremely adaptable materials with a wide variety of uses. They are desirable for use in catalytic processes and energy storage applications due to these qualities [73]. Fuel cells, hydrogen storage, lithium-ion batteries, and supercapacitors are a few examples of energy storage systems where MXenes are useful [74]– [77]. They also

show promising outcomes in areas including flexible electronics, optoelectronics, body-worn technology, and other biomedical and environmental applications.

There is increased interest in renewable energy sources and energy conversion technologies as a result of the exhaustion of fossil fuels and the rise in energy needs [78]. Due to their improved power densities and specific capacitance, lithium-ion batteries and supercapacitors in particular are attracting interest because they are well suited for compact and integrated applications like mobile phones, tablets, automotive systems, and other power sources. Supercapacitors, which might be used as a substitute to standard cells for energy storage because of their superior charge/discharge rates and process stability, present a tempting use for MXenes as a material.

In a basic KOH electrolytic solution, multilayered Ti3C2Tx, which has been investigated as a supercapacitor material, displays a specific capacitance of 340 F cm-2 [79]. Furthermore, Ti3C2Tx thin-film electrodes have outstanding process stability even after 10,000 cycles, exhibiting a volumetric capacitance of 900 F cm-3 at a scan rate of 20 mV/s [80]. These results show how interesting MXenes are for developing energy storage and exchange systems.

MXenes exhibit distinct charge/discharge mechanisms in different electrolytes, leading to varied behavior. In acidic electrolytes, $Ti_3C_2T_x$ mainly functions as a pseudocapacitor, while in neutral or alkaline electrolytes, it behaves as a double-layer capacitor, although with reduced performance. Recurrent redox events taking place close to the electrode's surface are the main cause of the pseudocapacitance. In contrast to double-layer capacitance, which depends on reversible electrolyte ion buildup without redox reactions (physical adsorption process), MXene-based pseudocapacitors as a result have large energy concentrations. Compared to aqueous or alkaline electrolytes, MXenes function electrochemically better in acidic electrolytes.

Since surface metrics directly affect the volumetric capacitance, the surface chemistry of MXenes has a substantial impact on its supercapacitor capabilities. Specific capacitance is improved by surface termination with F or O functional groups. Particularly in acidic electrolytes, chemical alterations during MXene production utilizing DMSO, KOH, NH4, or heat treatment significantly boost specific capacitance. MXenes like Mo_2CT_x and $Mo_{1.33}CT_x$ likewise showed encouraging supercapacitor performance, with $Mo_{1.33}CT_x$ exhibiting a 65% higher specific capacitance than Mo_2CT_x, attributed to the beneficial effect of vacancies. MXenes' flake size has been connected to particular capacitance, but more experimental confirmation is required [81].

Through hydrogen bonding and van der Waals forces, MXenes often accumulate, resulting in limited ion exchange and accessibility due to reduced surface area. However, these limitations can be addressed using macroporous structures, hydrogels, aligned crystalline structures, and new architectural designs. For example, $Ti_3C_2T_x$-polypyrrole nanocomposite and $(Mo_{2/3}Y_{1/3})CTx$ and $Ti_3C_2T_x$ hydrogels have been reported, exhibiting specific capacitance values of 1000 F cm^{-2} and above [82].

MXenes show potential as electrode materials for Li-ion batteries, which are often utilized in portable electronic devices for power and energy storage. Compared to typical materials like graphite, they provide better electrical conductivity and a particular surface area that enables effective Li storing at lower circuit voltages [83]. MXenes such as $Ti_3C_2T_x$ thin film have demonstrated gravimetric capacity over 410 mg/g, similar to Mo_2CT_x (423 mg/g) [84]. Nb_2CT_x and V_2CT_x are two MXenes for Li-ion storage that are currently known, with MXenes based on Cr, Zr, and Mn being some additional theoretically viable choices. [84], [85].

Despite the fact that there has been a lot of study on $Ti_3C_2T_x$, theoretical observations suggest that MXenes with lower stoichiometric indexes (M_4X_3, M_3X_3, and M_2X) exhibit increased gravimetric capacities[86]. For instance, Ti_2C demonstrated a 50% higher Li^+ gravimetric capacity compared to Ti_3C_2 [87]. Monolayered MXenes generally exhibit

higher gravimetric capacities than multilayers due to maximum Li adsorption during intercalation.

The storage capacity, intercalation, and operational potential of metallic ions are all significantly impacted by the presence of functional groups in MXenes. The diffusion barrier is further enhanced by the presence of F and OH terminal groups. For instance, the presence of OH termination substantially doubles the Li-ion capacity of Ti3C2Tx [88]. Additionally, conceptual investigations show that O termination increases capacity for storage [89]. The most promising MXene anode materials for Li-ion batteries are thought to be O-terminated pure M_2C compounds with light transition metals. The HCl - LiF synthesis approach is chosen over HF procedures to increase MXene capacity. Fewer F and OH terminations, fewer structural flaws, and a better delamination ratio arise from HCl-LiF synthesis, which improves electrochemical performance [90]. Hence, a synthesis route that allows better control over surface chemistry significantly contributes to improving MXene's electrochemical performance.

4.2. Gas sensing and Biosensing: -

For the sake of environmental and human safety in a variety of applications, sensory instruments are essential for monitoring substance concentrations. Minimal detection limit, excellent sensitivity, quick response, vast linear range, and great selectivity for certain analytes are success requirements for sensing devices. Additionally, cost-effectiveness is essential to facilitate easy commercialization. MXenes have fascinating characteristics that make them appropriate for use in sensing device applications. For instance, it has been demonstrated that MXene-derived quantum dots are capable of selectively quenching the light emission of Zn ions in the presence of different metal ions, making them useful for the creation of Zn^{2+} sensors [91].

In gas sensing applications, selective absorption and reversible release and capture of gases are critical. Ti_2C nanolayers have demonstrated excellent sensing ability for NH_3 due to the strategic positioning of N atoms above the Ti atoms in Ti_2CO_2nanolayers,

leading to stronger bonding through larger binding forces compared to other gases like CO, CO_2, H_2, CH_4, NO_2, and N_2 [92]. When bidirectional stresses are reduced, MXene monolayers may effectively release NH3, and following adsorption, MXenes show improved electrical conductivity [93]. O-terminated MXenes offer reversible NH_3 adsorption, and M_2CO_2 MXenes (where M represents, Hf, Zr, Sc, and Ti) have been investigated for gas-sensing applications [94]. Chemical adsorption on M2CO2 with charge transfer is the mechanism of NH3 adsorption, which allows for control of NH3 adsorption [93]. The reversible behavior of NH3 adsorption is caused by a change from chemical adsorption to physical adsorption which is enabled by an increase in adsorption energy. As potential options for gas sensing and capture applications, O-terminated MXenes seem promising.

Composites based on MXene have shown promise in their ability to detect macromolecules, cells, gases, and tiny molecules. For instance, Ti_3C_2 quantum dots with 10% quantum yields in photoluminescence were produced by a straightforward hydrothermal process at temperatures of 100, 120, and 150°C [95]. These quantum dots were utilized for cellular probing in vitro bioimaging of RAW 264.7 cells [96]. MXenes have also been successfully used for sensing cerebral activity by combining them with field-effect transistors in ultrathin conductive sheets [97]. Through π-π interactions between dopamine molecules and electrons from MXene termination groups (O, H, or F), the neurotransmitter dopamine was detected using this system. Real-time monitoring of primary hippocampal neurons in culture was also made possible by the sensing device, demonstrating great biocompatibility over an extended period of culture.

MXenes in general have enormous potential for use in the creation of sensing apparatus for a variety of purposes, such as environmental monitoring and biological detection. This is due to their outstanding conductivity, hydrophilicity, and biocompatibility, which make them highly versatile and suitable for various sensing applications.

4.3. Remediation of Environmental Pollutants: -

The ability of MXenes to absorb numerous toxic contaminants, including as lead (II), uranyl, chromium (VI), ammonia, copper, methylene blue, mercury, methane, and phosphate, has been well studied. Ti_3C_2 and $Ti_3C_2T_x$ are among the MXenes commonly used for environmental remediation. It has been discovered that $Ti_3C_2(OH/ONa)_xF_{2-x}$ MXene [98], produced by chemical exfoliation followed by alkalization intercalation, can absorb more Pb(II) than other divalent ions like Ca(II) and Mg(II) in a water-based solution. This phenomenon is ascribed to the MXenes' increased Ti2O bond affinity for Pb (II), which encourages the development of inner-space complexes.

The redox properties of 2D $Ti_3C_2T_x$ have been utilized for the effective removal of toxic water pollutants, such as Cr(VI) [99]. Water may be made safe for drinking by converting extremely harmful Cr(VI) to less toxic Cr(III) with the use of MXene. Additionally, $Ti_3C_2T_x$ mixed with $KMnO_4$ has been demonstrated to aid in the removal of Cu from water, outperforming commercially available activated carbon [100].

$Ti_3C_2OH_{0.8}F_{1.2}/Fe_2O_3$ nanocomposite has shown promise for phosphate removal through adsorption [101]. Due to the distribution of Fe_3O_4 on the MXene surface, which enables magnetic separation and enhances the ability to adsorb, the integration of MXene with Fe_2O_3 boosts the sorption capability.

Particularly Ti3C2Tx, which can absorb and degrade organic molecules in aqueous media under UV irradiation, MXenes also have strong sorption capabilities for eliminating colors and hazardous industrial pollutants from water. [102]. The negatively charged surface of MXenes facilitates electrostatic interactions, leading to the efficient removal of methylene blue. Under UV light, MXenes show outstanding adsorbent capacity for water purification, removing both methylene blue and AB80 dyes from water solutions [103].

Overall, MXenes hold great potential as effective tools for environmental remediation, providing solutions for water purification and pollutant removal in various applications

4.4. Applications in Medical and Biomedical: -

MXenes are excellent for anticancer treatments and bioimaging applications due to their distinct characteristics. Common limitations of traditional cancer therapies like radiation and chemotherapy include non-specificity and unfavorable side effects. Hence, there is a need for more effective and compatible treatment methods. By utilizing photothermal agents, a light-controlled method for targeting and destroying tumor cells, photothermal treatment offers the potential to improve selectivity. [104].

Numerous nanomaterials have been investigated for photothermal treatment, including copper sulfide nanoparticles, black phosphorus, gold nanorods, and nanomaterials based on carbon. MXenes, particularly $Ti_3C_2T_x$ with near-infrared (NIR) absorption capabilities following Al-oxyanion termination, have also emerged as potential photothermal therapy agents [105]. As photothermal therapies against murine breast cancer, $Ti_3C_2T_x$ sheets with OH or F termination have in particular shown encouraging results.

It has been suggested to use MnO_x/Ti_3C_2 composite for bioimaging and photothermal treatments [106]. Following infrared laser irradiation, the composite's surface was modified using soybean phospholipids, which effectively killed cancer cells and reduced tumor development [107].

After being injected intravenously into animals at low doses, MXene quantum dots demonstrated great photothermal conversion efficiency, making them efficient in killing cervical cancer cells in vivo and in vitro. [108].

To create Ti3C2-BG scaffolds, researchers combined Ti3C2 MXene with 3D-printed bioactive glass scaffolds [109]. These scaffolds had a high photothermal conversion efficiency, which resulted in photothermal hyperthermia that eliminated the tumor and promoted the formation of newly formed bone tissue in vivo. These composite scaffolds are very desirable for the treatment of bone tumors due to their dual activity.

In summary, MXenes offer promising prospects for enhancing cancer therapies through photothermal therapy, and their unique properties make them versatile candidates for both cancer treatment and bioimaging applications.

5. OVERCOMING OBSTACLES AND EMBRACING POSSIBILITIES

MXenes, a brand-new family of 2D materials with exceptional characteristics, have a wide range of possible uses. The majority of the study has been theoretical, lacking experimental validation despite their remarkable mechanical, electrical, optical, and magnetic properties. However, the focus has shifted towards exploring specific applications. Delamination procedures with suitable surface terminations have shown promising results for energy storage, catalysis, and EMI shielding applications. The synthesis and surface termination techniques have a substantial influence on the characteristics of MXene. Further research is needed to optimize MXene surface functionalization for improved chemical applicability.

Combining experimental and theoretical approaches will be essential to uncover MXenes' complex properties and meet future demands. Research continuity is essential, particularly for the identification of missing MAX phases like Ti3AlN2 and Ti2SiC, as well as for the investigation of new MXenes with thermally stable stoichiometries, superconductive behavior, and unique magnetic aspects. Efforts to narrow the theoretical and experimental gap and explore the effect of doping on MAX phases for tunable conductivity should be intensified. Understanding the anisotropy in electronic properties through momentum dependence measurements will further enhance our comprehension of MAX phases.

The advancement of MXene applications will also depend on the development of cutting-edge synthesis and material processing techniques for corrosion- and oxidation-resistant MAX phases that have minimal resistance and outstanding durability.

In conclusion, a multidisciplinary approach incorporating both theoretical and experimental techniques is essential for realizing MXenes' full potential and uncovering fresh applications for them in a variety of technological problems.

REFERENCES: -

[1] C. Tan *et al.*, "Recent Advances in Ultrathin Two-Dimensional Nanomaterials," *Chem Rev*, vol. 117, no. 9, pp. 6225–6331, May 2017, doi: 10.1021/ACS.CHEMREV.6B00558.

[2] V. Nicolosi, M. Chhowalla, M. G. Kanatzidis, M. S. Strano, and J. N. Coleman, "Liquid Exfoliation of Layered Materials," *Science (1979)*, vol. 340, no. 6139, 2013, doi: 10.1126/SCIENCE.1226419.

[3] K. S. Novoselov*et al.*, "Two-dimensional atomic crystals," *Proc Natl Acad Sci U S A*, vol. 102, no. 30, pp. 10451–10453, Jul. 2005, doi: 10.1073/PNAS.0502848102.

[4] M. Naguib *et al.*, "Two-Dimensional Nanocrystals Produced by Exfoliation of Ti3AlC2," *Advanced Materials*, vol. 23, no. 37, pp. 4248–4253, Oct. 2011, doi: 10.1002/ADMA.201102306.

[5] K. Nabeela and N. B. Sumina, *MXenes and their composites as piezoresistive sensors*. Elsevier, 2021. doi: 10.1016/B978-0-12-823361-0.00011-3.

[6] R. M. Ronchi, J. T. Arantes, and S. F. Santos, "Synthesis, structure, properties and applications of MXenes: Current status and perspectives," *Ceram Int*, vol. 45, no. 15, pp. 18167–18188, Oct. 2019, doi: 10.1016/J.CERAMINT.2019.06.114.

[7] M. W. Barsoum, "The MN+1AXN phases: A new class of solids: Thermodynamically stable nanolaminates," *Progress in Solid State Chemistry*, vol. 28, no. 1–4, pp. 201–281, Jan. 2000, doi: 10.1016/S0079-6786(00)00006-6.

[8] B. Anasori, M. R. Lukatskaya, and Y. Gogotsi, "2D metal carbides and nitrides (MXenes) for energy storage," *Nat Rev Mater*, vol. 2, no. 2, Jan. 2017, doi: 10.1038/NATREVMATS.2016.98.

[9] P. O. Å. Persson and J. Rosen, "Current state of the art on tailoring the MXene composition, structure, and surface chemistry," *CurrOpin Solid State Mater Sci*, vol. 23, no. 6, Dec. 2019, doi: 10.1016/J.COSSMS.2019.100774.

[10] M. Naguib, V. N. Mochalin, M. W. Barsoum, and Y. Gogotsi, "25th-anniversary article: MXenes: a new family of two-dimensional materials," *Adv Mater*, vol. 26, no. 7, pp. 992–1005, Feb. 2014, doi: 10.1002/ADMA.201304138.

[11] J. Zhu *et al.*, "Recent advance in MXenes: A promising 2D material for catalysis, sensor, and chemical adsorption," *Coord Chem Rev*, vol. 352, pp. 306–327, Dec. 2017, doi: 10.1016/J.CCR.2017.09.012.

[12] B. Zhou *et al.*, "Flexible, Robust, and Multifunctional Electromagnetic Interference Shielding Film with Alternating Cellulose Nanofiber and MXene Layers," *ACS Appl Mater Interfaces*, vol. 12, no. 4, pp. 4895–4905, Jan. 2020, doi: 10.1021/ACSAMI.9B19768/SUPPL_FILE/AM9B19768_SI_001.PDF.

[13] P. Eklund, J. Rosen, and P. O. Å. Persson, "Layered ternary Mn+1AXn phases and their 2D derivative MXene: An overview from a thin-film perspective," *J Phys D Appl Phys*, vol. 50, no. 11, Feb. 2017, doi: 10.1088/1361-6463/AA57BC.

[14] M. Khazaei*et al.*, "Novel Electronic and Magnetic Properties of Two-Dimensional Transition Metal Carbides and Nitrides," *Adv Funct Mater*, vol. 23, no. 17, pp. 2185–2192, May 2013, doi: 10.1002/ADFM.201202502.

[15] T. Hu, J. Wang, H. Zhang, Z. Li, M. Hu, and X. Wang, "Vibrational properties of Ti_3C_2 and $Ti_3C_2T_2$ (T = O, F, OH) monosheets by first-principles calculations: a comparative study," *Physical Chemistry Chemical Physics*, vol. 17, no. 15, pp. 9997–10003, Apr. 2015, doi: 10.1039/C4CP05666C.

[16] J. L. Hart *et al.*, "Control of MXenes' electronic properties through termination and intercalation," *Nat Commun*, vol. 10, no. 1, Dec. 2019, doi: 10.1038/S41467-018-08169-8.

[17] J. Halim *et al.*, "Transparent Conductive Two-Dimensional Titanium Carbide Epitaxial Thin Films," *Chem Mater*, vol. 26, no. 7, pp. 2374–2381, Apr. 2014, doi: 10.1021/CM500641A.

[18] X. Sang *et al.*, "Atomic Defects in Monolayer Titanium Carbide ($Ti_3C_2T_x$) MXene," *ACS Nano*, vol. 10, no. 10, pp. 9193–9200, Oct. 2016, doi: 10.1021/ACSNANO.6B05240.

[19] M. Alhabeb*et al*, "Guidelines for Synthesis and Processing of Two-Dimensional Titanium Carbide ($Ti_3C_2T_x$MXene)," *Chemistry of Materials*, vol. 29, no. 18, pp. 7633–7644, Sep. 2017, doi: 10.1021/ACS.CHEMMATER.7B02847.

[20] Y. Gogotsi, "Chemical vapor deposition: Transition metal carbides go 2D," *Nat Mater*, vol. 14, no. 11, pp. 1079–1080, Nov. 2015, doi: 10.1038/NMAT4386.

[21] L. Li, "Lattice dynamics and electronic structures of $Ti_3C_2O_2$ and $Mo_2TiC_2O_2$ (MXenes): The effect of Mo substitution," *Comput Mater Sci*, vol. 124, pp. 8–14, Nov. 2016, doi: 10.1016/J.COMMATSCI.2016.07.008.

[22] M. Khazaei*et al.*, "Nearly free electron states in MXenes," *Phys Rev B*, vol. 93, no. 20, p. 205125, May 2016, doi: 10.1103/PHYSREVB.93.205125/FIGURES/6/MEDIUM.

[23] T. Hu, J. Yang, and X. Wang, "Carbon vacancies in Ti2CT2 MXenes: defects or a new opportunity?" *Physical Chemistry Chemical Physics*, vol. 19, no. 47, pp. 31773–31780, Dec. 2017, doi: 10.1039/C7CP06593K.

[24] J. Xu *et al.*, "MXene Electrode for the Integration of WSe_2 and MoS_2 Field Effect Transistors," *Adv Funct Mater*, vol. 26, no. 29, pp. 5328–5334, Aug. 2016, doi: 10.1002/ADFM.201600771.

[25] J. Halim *et al.*, "Transparent Conductive Two-Dimensional Titanium Carbide Epitaxial Thin Films," *Chem Mater*, vol. 26, no. 7, pp. 2374–2381, Apr. 2014, doi: 10.1021/CM500641A.

[26] M. Naguib *et al.*, "Two-dimensional transition metal carbides," *ACS Nano*, vol. 6, no. 2, pp. 1322–1331, Feb. 2012, doi: 10.1021/NN204153H.

[27] J. Halim *et al.*, "Transparent Conductive Two-Dimensional Titanium Carbide Epitaxial Thin Films," *Chem Mater*, vol. 26, no. 7, pp. 2374–2381, Apr. 2014, doi: 10.1021/CM500641A.

[28] B. Anasori*et al.*, "Control of electronic properties of 2D carbides (MXenes) by manipulating their transition metal layers," *Nanoscale Horiz*, vol. 1, no. 3, pp. 227–234, Apr. 2016, doi: 10.1039/C5NH00125K.

[29] Q. Tao *et al.*, "Two-dimensional $Mo_{1.33}C$ MXene with divacancy ordering prepared from parent 3D laminate with in-plane chemical ordering," *Nat Commun*, vol. 8, 2017, doi: 10.1038/NCOMMS14949.

[30] A. D. Dillon *et al.*, "Highly Conductive Optical Quality Solution-Processed Films of 2D Titanium Carbide," *Adv Funct Mater*, vol. 26, no. 23, pp. 4162–4168, Jun. 2016, doi: 10.1002/ADFM.201600357.

[31] F. Shahzad *et al.*, "Electromagnetic interference shielding with 2D transition metal carbides (MXenes)," *Science*, vol. 353, no. 6304, pp. 1137–1140, Sep. 2016, doi: 10.1126/SCIENCE.AAG2421.

[32] T. Hu, J. Wang, H. Zhang, Z. Li, M. Hu, and X. Wang, "Vibrational properties of Ti_3C_2 and $Ti_3C_2T_2$ (T = O, F, OH) nanosheets by first-principles calculations: a comparative study," *Physical Chemistry Chemical Physics*, vol. 17, no. 15, pp. 9997–10003, Apr. 2015, doi: 10.1039/C4CP05666C.

[33] J. L. Hart *et al.*, "Control of MXenes' electronic properties through termination and intercalation," *Nat Commun*, vol. 10, no. 1, Dec. 2019, doi: 10.1038/S41467-018-08169-8.

[34] J. Halim *et al.*, "Transparent Conductive Two-Dimensional Titanium Carbide Epitaxial Thin Films," *Chem Mater*, vol. 26, no. 7, pp. 2374–2381, Apr. 2014, doi: 10.1021/CM500641A.

[35] A. D. Dillon *et al.*, "Highly Conductive Optical Quality Solution-Processed Films of 2D Titanium Carbide," *Adv Funct Mater*, vol. 26, no. 23, pp. 4162–4168, Jun. 2016, doi: 10.1002/ADFM.201600357.

[36] T. Hu, J. Yang, and X. Wang, "Carbon vacancies in Ti_2CT_2MXenes: defects or a new opportunity?" *Physical Chemistry Chemical Physics*, vol. 19, no. 47, pp. 31773–31780, Dec. 2017, doi: 10.1039/C7CP06593K.

[37] S. Huang, K. C. Mutyala, A. V. Sumant, and V. N. Mochalin, "Achieving superlubricity with 2D transition metal carbides (MXenes) and MXene/graphene coatings," *Mater Today Adv*, vol. 9, p. 100133, Mar. 2021, doi: 10.1016/J.MTADV.2021.100133.

[38] B. Yorulmaz, A. Özden, H. Şar, F. Ay, C. Sevik, and N. K. Perkgöz, "CVD growth of monolayer WS_2 through controlled seed formation and vapor density," *Mater Sci Semicond Process*, vol. 93, pp. 158–163, Apr. 2019, doi: 10.1016/J.MSSP.2018.12.035.

[39] Z. Guo, J. Zhou, C. Si, and Z. Sun, "Flexible two-dimensional $Ti_{n+1}C_n$ (n = 1, 2 and 3) and their functionalized MXenes predicted by density functional theories," *Physical Chemistry Chemical Physics*, vol. 17, no. 23, pp. 15348–15354, Jun. 2015, doi: 10.1039/C5CP00775E.

[40] A. Lipatov*et al.*, "Elastic properties of 2D $Ti_3C_2T_x$MXene monolayers and bilayers," *Sci Adv*, vol. 4, no. 6, Jun. 2018, doi: 10.1126/SCIADV.AAT0491.

[41] Z. Ling *et al.*, "Flexible and conductive MXene films and nanocomposites with high capacitance," *Proc Natl Acad Sci USA*, vol. 111, no. 47, pp. 16676–16681, Nov. 2014, doi: 10.1073/PNAS.1414215111.

[42] W. Tian *et al.*, "Multifunctional Nanocomposites with High Strength and Capacitance Using 2D MXene and 1D Nanocellulose," *Adv Mater*, vol. 31, no. 41, Oct. 2019, doi: 10.1002/ADMA.201902977.

[43] J. Come *et al.*, "Nanoscale Elastic Changes in 2D $Ti_3C_2T_x$ (MXene) Pseudocapacitive Electrodes," *Adv Energy Mater*, vol. 6, no. 9, May 2016, doi: 10.1002/AENM.201502290.

[44] T. Hu, J. Yang, W. Li, X. Wang, and C. M. Li, "Quantifying the rigidity of 2D carbides (MXenes)," *Physical Chemistry Chemical Physics*, vol. 22, no. 4, pp. 2115–2121, Jan. 2020, doi: 10.1039/C9CP05412J.

[45] K. Li *et al.*, "An Ultrafast Conducting Polymer@MXene Positive Electrode with High Volumetric Capacitance for Advanced Asymmetric Supercapacitors," *Small*, vol. 16, no. 4, p. 1906851, Jan. 2020, doi: 10.1002/SMLL.201906851.

[46] C. J. Zhang *et al.*, "Oxidation Stability of Colloidal Two-Dimensional Titanium Carbides (MXenes)," *Chemistry of Materials*, vol. 29, no. 11, pp. 4848–4856, Jun. 2017, doi: 10.1021/ACS.CHEMMATER.7B00745.

[47] X. Zhao *et al.*, "Antioxidants Unlock Shelf-Stable Ti_3C_2T (MXene) Nanosheet Dispersions," *Matter*, vol. 1, no. 2, pp. 513–526, Aug. 2019, doi: 10.1016/J.MATT.2019.05.020.

[48] B. Anasori, M. R. Lukatskaya, and Y. Gogotsi, "2D metal carbides and nitrides (MXenes) for energy storage," *Nat Rev Mater*, vol. 2, no. 2, Jan. 2017, doi: 10.1038/NATREVMATS.2016.98.

[49] B. Ahmed, D. H. Anjum, Y. Gogotsi, and H. N. Alshareef, "Atomic layer deposition of SnO_2 on MXene for Li-ion battery anodes," *Nano Energy*, vol. 34, pp. 249–256, Apr. 2017, doi: 10.1016/J.NANOEN.2017.02.043.

[50] Q. Xue*et al.*, "Photoluminescent Ti_3C_2MXene Quantum Dots for Multicolor Cellular Imaging," *Advanced Materials*, vol. 29, no. 15, p. 1604847, Apr. 2017, doi: 10.1002/ADMA.201604847.

[51] K. Zhong *et al.*, "A novel near-infrared fluorescent probe for highly selective recognition of hydrogen sulfide and imaging in living cells," *RSC Adv*, vol. 8, no. 42, pp. 23924–23929, Jun. 2018, doi: 10.1039/C8RA03457E.

[52] R. Thakur *et al.*, "Insights into the thermal and chemical stability of multilayered V_2CT_xMXene," *Nanoscale*, vol. 11, no. 22, pp. 10716–10726, Jun. 2019, doi: 10.1039/C9NR03020D.

[53] N. K. Chaudhari, H. Jin, B. Kim, D. San Baek, S. H. Joo, and K. Lee, "MXene: an emerging two-dimensional material for future energy conversion and storage applications," *J Mater Chem A Mater*, vol. 5, no. 47, pp. 24564–24579, Dec. 2017, doi: 10.1039/C7TA09094C.

[54] J. Come *et al.*, "Controlling the actuation properties of MXene paper electrodes upon cation intercalation," *Nano Energy*, vol. 17, pp. 27–35, 2015, doi: 10.1016/J.NANOEN.2015.07.028.

[55] J. N. Coleman *et al.*, "Two-dimensional nanosheets produced by liquid exfoliation of layered materials," *Science*, vol. 331, no. 6017, pp. 568–571, Feb. 2011, doi: 10.1126/SCIENCE.1194975.

[56] O. Mashtalir, M. Naguib, B. Dyatkin, Y. Gogotsi, and M. W. Barsoum, "Kinetics of aluminum extraction from Ti_3AlC_2 in hydrofluoric acid," *Mater Chem Phys*, vol. 139, no. 1, pp. 147–152, Apr. 2013, doi: 10.1016/J.MATCHEMPHYS.2013.01.008.

[57] M. Naguib *et al.*, "One-step synthesis of nanocrystalline transition metal oxides on thin sheets of disordered graphitic carbon by oxidation of MXenes," *Chemical Communications*, vol. 50, no. 56, pp. 7420–7423, Jun. 2014, doi: 10.1039/C4CC01646G.

[58] Y. Pei *et al.*, "$Ti_3C_2T_X$MXene for Sensing Applications: Recent Progress, Design Principles, and Future Perspectives," *ACS Nano*, vol. 15, no. 3, pp. 3996–4017, Mar. 2021, doi: 10.1021/ACSNANO.1C00248.

[59] A. Lipatov, M. Alhabeb, M. R. Lukatskaya, A. Boson, Y. Gogotsi, and A. Sinitskii, "MXene Materials: Effect of Synthesis on Quality, Electronic Properties and Environmental Stability of Individual Monolayer Ti_3C_2MXene Flakes (Adv. Electron. Mater. 12/2016)," *Adv Electron Mater*, vol. 2, no. 12, Dec. 2016, doi: 10.1002/AELM.201670068.

[60] F. Liu *et al.*, "Preparation of Ti3C2 and Ti2C MXenes by fluoride salts etching and methane adsorptive properties," *Appl Surf Sci*, vol. 416, pp. 781–789, Sep. 2017, doi: 10.1016/J.APSUSC.2017.04.239.

[61] X. Wang *et al.*, "A new etching environment (FeF_3/HCl) for the synthesis of two-dimensional titanium carbide MXenes: a route towards selective reactivity vs. water," *J Mater Chem A Mater*, vol. 5, no. 41, pp. 22012–22023, Oct. 2017, doi: 10.1039/C7TA01082F.

[62] M. Alhabeb*et al.*, "Guidelines for Synthesis and Processing of Two-Dimensional Titanium Carbide ($Ti_3C_2T_x$MXene)," *Chemistry of Materials*, vol. 29, no. 18, pp. 7633–7644, Sep. 2017, doi: 10.1021/ACS.CHEMMATER.7B02847.

[63] X. Zhang, Y. Yang, and Z. Zhou, "Towards practical lithium-metal anodes," *Chem Soc Rev*, vol. 49, no. 10, pp. 3040–3071, May 2020, doi: 10.1039/C9CS00838A.

[64] M. Mariano *et al.*, "Solution-processed titanium carbide MXene films examined as highly transparent conductors," *Nanoscale*, vol. 8, no. 36, pp. 16371–16378, Sep. 2016, doi: 10.1039/C6NR03682A.

[65] Y. Y. Peng *et al.*, "All-MXene (2D titanium carbide) solid-state microsupercapacitors for on-chip energy storage," *Energy Environ Sci*, vol. 9, no. 9, pp. 2847–2854, Aug. 2016, doi: 10.1039/C6EE01717G.

[66] L. Zhang *et al.*, "MXene coupled with molybdenum dioxide nanoparticles as 2D-0D pseudocapacitive electrode for high performance flexible asymmetric micro-supercapacitors," *Journal of Materiomics*, vol. 6, no. 1, pp. 138–144, Mar. 2020, doi: 10.1016/J.JMAT.2019.12.013.

[67] E. Quain*et al.*, "Direct Writing of Additive-Free MXene-in-Water Ink for Electronics and Energy Storage," *Adv Mater Technol*, vol. 4, no. 1, Jan. 2018, doi: 10.1002/ADMT.201800256.

[68] A. Lerf and R. Schöllhorn, "Solvation Reactions of Layered Ternary Sulfides A_xTiS_2, A_xNbS_2, and A_xTaS_2," *Inorg Chem*, vol. 16, no. 11, pp. 2950–2956, Nov. 1977, doi: 10.1021/IC50177A057/ASSET/IC50177A057.FP.PNG_V03.

[69] M. Ghidiu, J. Halim, S. Kota, D. Bish, Y. Gogotsi, and M. W. Barsoum, "Ion-Exchange and Cation Solvation Reactions in Ti_3C_2MXene," *Chemistry of Materials*, vol. 28, no. 10, pp. 3507–3514, May 2016, doi: 10.1021/ACS.CHEMMATER.6B01275/SUPPL_FILE/CM6B01275_SI_001.PDF.

[70] J. Xuan *et al.*, "Organic-Base-Driven Intercalation and Delamination for the Production of Functionalized Titanium Carbide Nanosheets with Superior Photothermal Therapeutic Performance," *Angew Chem Int Ed Engl*, vol. 55, no. 47, pp. 14569–14574, Nov. 2016, doi: 10.1002/ANIE.201606643.

[71] X. Yu, X. Cai, H. Cui, S. W. Lee, X. F. Yu, and B. Liu, "Fluorine-free preparation of titanium carbide MXene quantum dots with high near-infrared photothermal performances for cancer therapy," *Nanoscale*, vol. 9, no. 45, pp. 17859–17864, Dec. 2017, doi: 10.1039/C7NR05997C.

[72] T. Li *et al.*, "Fluorine-Free Synthesis of High-Purity $Ti_3C_2T_x$ (T=OH, O) via Alkali Treatment," *Angew Chem Int Ed Engl*, vol. 57, no. 21, pp. 6115–6119, May 2018, doi: 10.1002/ANIE.201800887.

[73] R. M. Ronchi, J. T. Arantes, and S. F. Santos, "Synthesis, structure, properties and applications of MXenes: Current status and perspectives," *Ceram Int*, vol. 45, no. 15, pp. 18167–18188, Oct. 2019, doi: 10.1016/J.CERAMINT.2019.06.114.

[74] B. Anasori, M. R. Lukatskaya, and Y. Gogotsi, "2D metal carbides and nitrides (MXenes) for energy storage," *Nat Rev Mater*, vol. 2, no. 2, Jan. 2017, doi: 10.1038/NATREVMATS.2016.98.

[75] M. Naguib, V. N. Mochalin, M. W. Barsoum, and Y. Gogotsi, "25th anniversary article: MXenes: a new family of two-dimensional materials," *Adv Mater*, vol. 26, no. 7, pp. 992–1005, Feb. 2014, doi: 10.1002/ADMA.201304138.

[76] J. C. Lei, X. Zhang, and Z. Zhou, "Recent advances in MXene: Preparation, properties, and applications," *Front Phys (Beijing)*, vol. 10, no. 3, pp. 276–286, Jun. 2015, doi: 10.1007/S11467-015-0493-X.

[77] L. Wang *et al.*, "Synthesis and electrochemical performance of $Ti_3C_2T_x$ with hydrothermal process," *Electronic Materials Letters*, vol. 12, no. 5, pp. 702–710, Sep. 2016, doi: 10.1007/S13391-016-6088-Z/METRICS.

[78] J. Pang *et al.*, "Applications of 2D MXenes in energy conversion and storage systems," *Chem Soc Rev*, vol. 48, no. 1, pp. 72–133, Jan. 2019, doi: 10.1039/C8CS00324F.

[79] M. R. Lukatskaya*et al.*, "Cation intercalation and high volumetric capacitance of two-dimensional titanium carbide," *Science*, vol. 341, no. 6153, pp. 1502–1505, 2013, doi: 10.1126/SCIENCE.1241488.

[80] M. Ghidiu, M. R. Lukatskaya, M. Q. Zhao, Y. Gogotsi, and M. W. Barsoum, "Conductive two-dimensional titanium carbide 'clay' with high volumetric capacitance," *Nature*, vol. 516, no. 7529, pp. 78–81, Dec. 2014, doi: 10.1038/NATURE13970.

[81] E. Kayali, A. Vahidmohammadi, J. Orangi, and M. Beidaghi, "Controlling the Dimensions of 2D MXenes for Ultrahigh-Rate Pseudocapacitive Energy Storage," *ACS Appl Mater Interfaces*, vol. 10, no. 31, pp. 25949–25954, Aug. 2018, doi: 10.1021/ACSAMI.8B07397.

[82] M. R. Lukatskaya*et al.*, "Ultra-high-rate pseudocapacitive energy storage in two-dimensional transition metal carbides," *Nat Energy*, vol. 6, Jul. 2017, doi: 10.1038/NENERGY.2017.105.

[83] J. Pang *et al.*, "Applications of 2D MXenes in energy conversion and storage systems," *Chem Soc Rev*, vol. 48, no. 1, pp. 72–133, Jan. 2019, doi: 10.1039/C8CS00324F.

[84] K. Hantanasirisakul and Y. Gogotsi, “Electronic and Optical Properties of 2D Transition Metal Carbides and Nitrides (MXenes),” *Adv Mater*, vol. 30, no. 52, Dec. 2018, doi: 10.1002/ADMA.201804779.

[85] V. Ming *et al.*, “Correction: Recent progress in layered transition metal carbides and/or nitrides (MXenes) and their composites: synthesis and applications,” *J Mater Chem A Mater*, vol. 5, no. 18, pp. 8769–8769, May 2017, doi: 10.1039/C7TA90088K.

[86] C. Eames and M. S. Islam, “Ion intercalation into two-dimensional transition-metal carbides: global screening for new high-capacity battery materials,” *J Am Chem Soc*, vol. 136, no. 46, pp. 16270–16276, Nov. 2014, doi: 10.1021/JA508154E.

[87] J. Zhu, A. Chroneos, J. Eppinger, and U. Schwingenschlögl, “S-functionalized MXenes as electrode materials for Li-ion batteries,” *Appl Mater Today*, vol. 5, pp. 19–24, Dec. 2016, doi: 10.1016/J.APMT.2016.07.005.

[88] Q. Tang, Z. Zhou, and P. Shen, “Are MXenes promising anode materials for Li-ion batteries? Computational studies on electronic properties and Li storage capability of Ti_3C_2 and $Ti_3C_2X_2$ (X = F, OH) monolayer,” *J Am Chem Soc*, vol. 134, no. 40, pp. 16909–16916, Oct. 2012, doi: 10.1021/JA308463R.

[89] Q. Tang, Z. Zhou, and P. Shen, “Are MXenes promising anode materials for Li-ion batteries? Computational studies on electronic properties and Li storage capability of Ti_3C_2 and $Ti_3C_2X_2$ (X = F, OH) monolayer,” *J Am Chem Soc*, vol. 134, no. 40, pp. 16909–16916, Oct. 2012, doi: 10.1021/JA308463R/SUPPL_FILE/JA308463R_SI_001.PDF.

[90] Z. Ling *et al.*, “Flexible and conductive MXene films and nanocomposites with high capacitance,” *Proc Natl Acad Sci U S A*, vol. 111, no. 47, pp. 16676–16681, Nov. 2014, doi: 10.1073/PNAS.1414215111.

[91] Q. Xue*et al.*, “Photoluminescent Ti3C2 MXene Quantum Dots for Multicolor Cellular Imaging,” *Advanced Materials*, vol. 29, no. 15, p. 1604847, Apr. 2017, doi: 10.1002/ADMA.201604847.

[92] A. Sinha *et al.*, “MXene: An emerging material for sensing and biosensing,” *TrAC Trends in Analytical Chemistry*, vol. 105, pp. 424–435, Aug. 2018, doi: 10.1016/J.TRAC.2018.05.021.

[93] X. F. Yu *et al.*, “Monolayer Ti2CO2: A Promising Candidate for NH3 Sensor or Capturer with High Sensitivity and Selectivity,” *ACS Appl Mater Interfaces*, vol. 7, no. 24, pp. 13707–13713, Jun. 2015, doi: 10.1021/ACSAMI.5B03737/SUPPL_FILE/AM5B03737_SI_001.PDF.

[94] B. Xiao, Y. C. Li, X. F. Yu, and J. B. Cheng, “MXenes: Reusable materials for NH3 sensor or capturer by controlling the charge injection,” *Sens Actuators B Chem*, vol. 235, pp. 103–109, Nov. 2016, doi: 10.1016/J.SNB.2016.05.062.

[95] Q. Xue*et al.*, "Photoluminescent Ti_3C_2MXene Quantum Dots for Multicolor Cellular Imaging," *Adv Mater*, vol. 29, no. 15, Apr. 2017, doi: 10.1002/ADMA.201604847.

[96] Q. Xue*et al.*, "Photoluminescent Ti_3CMXene Quantum Dots for Multicolor Cellular Imaging," *Advanced Materials*, vol. 29, no. 15, p. 1604847, Apr. 2017, doi: 10.1002/ADMA.201604847.

[97] B. Xu *et al.*, "Ultrathin MXene-Micropattern-Based Field-Effect Transistor for Probing Neural Activity," *Advanced Materials*, vol. 28, no. 17, pp. 3333–3339, May 2016, doi: 10.1002/ADMA.201504657.

[98] Q. Peng *et al.*, "Unique lead adsorption behavior of activated hydroxyl group in two-dimensional titanium carbide," *J Am Chem Soc*, vol. 136, no. 11, pp. 4113–4116, Mar. 2014, doi: 10.1021/JA500506K.

[99] Y. Ying *et al.*, "Two-dimensional titanium carbide for efficiently reductive removal of highly toxic chromium(VI) from water," *ACS Appl Mater Interfaces*, vol. 7, no. 3, pp. 1795–1803, Jan. 2015, doi: 10.1021/AM5074722.

[100] A. Shahzad *et al.*, "Two-Dimensional $Ti_3C_2T_x$MXene Nanosheets for Efficient Copper Removal from Water," *ACS Sustain Chem Eng*, vol. 5, no. 12, pp. 11481–11488, Dec. 2017, doi: 10.1021/ACSSUSCHEMENG.7B02695.

[101] Q. Zhang *et al.*, "Efficient phosphate sequestration for water purification by unique sandwich-like MXene/magnetic iron oxide nanocomposites," *Nanoscale*, vol. 8, no. 13, pp. 7085–7093, Mar. 2016, doi: 10.1039/C5NR09303A.

[102] O. Mashtalir, K. M. Cook, V. N. Mochalin, M. Crowe, M. W. Barsoum, and Y. Gogotsi, "Dye adsorption and decomposition on two-dimensional titanium carbide in aqueous media," *J Mater Chem A Mater*, vol. 2, no. 35, pp. 14334–14338, Sep. 2014, doi: 10.1039/C4TA02638A.

[103] A. Szuplewska*et al.*, "Future Applications of MXenes in Biotechnology, Nanomedicine, and Sensors," *Trends Biotechnol*, vol. 38, no. 3, pp. 264–279, Mar. 2020, doi: 10.1016/J.TIBTECH.2019.09.001.

[104] R. S. Riley and E. S. Day, "Gold nanoparticle-mediated photothermal therapy: applications and opportunities for multimodal cancer treatment," *Wiley Interdiscip Rev NanomedNanobiotechnol*, vol. 9, no. 4, Jul. 2017, doi: 10.1002/WNAN.1449.

[105] R. S. Riley and E. S. Day, "Gold nanoparticle-mediated photothermal therapy: applications and opportunities for multimodal cancer treatment," *Wiley Interdiscip Rev NanomedNanobiotechnol*, vol. 9, no. 4, Jul. 2017, doi: 10.1002/WNAN.1449.

[106] C. Dai, H. Lin, G. Xu, Z. Liu, R. Wu, and Y. Chen, "Biocompatible 2D Titanium Carbide (MXenes) Composite Nanosheets for pH-Responsive MRI-Guided Tumor Hyperthermia," *Chemistry of Materials*, vol. 29, no. 20, pp. 8637–8652, Oct. 2017, doi: 10.1021/ACS.CHEMMATER.7B02441/SUPPL_FILE/CM7B02441_SI_001.PDF.

[107] A. Szuplewska*et al.*, "Future Applications of MXenes in Biotechnology, Nanomedicine, and Sensors.," *Trends Biotechnol*, vol. 38, no. 3, pp. 264–279, Mar. 2020, doi: 10.1016/J.TIBTECH.2019.09.001.

[108] X. Yu, X. Cai, H. Cui, S. W. Lee, X. F. Yu, and B. Liu, "Fluorine-free preparation of titanium carbide MXene quantum dots with high near-infrared photothermal performances for cancer therapy," *Nanoscale*, vol. 9, no. 45, pp. 17859–17864, Nov. 2017, doi: 10.1039/C7NR05997C.

[109] S. Pan *et al.*, "2D MXene-Integrated 3D-Printing Scaffolds for Augmented Osteosarcoma Phototherapy and Accelerated Tissue Reconstruction," *Adv Sci (Weinh)*, vol. 7, no. 2, Jan. 2019, doi: 10.1002/ADVS.201901511.

[110] Y. Wang, Y. Xu, M. Hu, H. Ling, and X. Zhu, "MXenes: Focus on optical and electronic properties and corresponding applications," *Nanophotonics*, vol. 9, no. 7, pp. 1601–1620, Jul. 2020, doi: 10.1515/NANOPH-2019-0556/PDF.

[111] S. K. Nemani*et al.*, "High-Entropy 2D Carbide MXenes: $TiVNbMoC_3$ and $TiVCrMoC_3$," *ACS Nano*, vol. 15, no. 8, pp. 12815–12825, Aug. 2021, doi: 10.1021/ACSNANO.1C02775.

[112] Q. Tang, Z. Zhou, and P. Shen, "Are MXenes promising anode materials for Li ion batteries? Computational studies on electronic properties and Li storage capability of Ti_3C_2 and $Ti_3C_2X_2$ (X = F, OH) monolayer," *J Am Chem Soc*, vol. 134, no. 40, pp. 16909–16916, Oct. 2012, doi: 10.1021/JA308463R.

[113] T. Hu, J. Wang, H. Zhang, Z. Li, M. Hu, and X. Wang, "Vibrational properties of Ti_3C_2 and $Ti_3C_2T_2$ (T = O, F, OH) monosheets by first-principles calculations: a comparative study," *Physical Chemistry Chemical Physics*, vol. 17, no. 15, pp. 9997–10003, Apr. 2015, doi: 10.1039/C4CP05666C.

[114] O. Mashtalir*et al.*, "Intercalation and delamination of layered carbides and carbonitrides," *Nat Commun*, vol. 4, 2013, doi: 10.1038/NCOMMS2664.

[115] O. Mashtalir, M. R. Lukatskaya, M. Q. Zhao, M. W. Barsoum, and Y. Gogotsi, "Amine-Assisted Delamination of Nb_2C MXene for Li-Ion Energy Storage Devices," *Adv Mater*, vol. 27, no. 23, pp. 3501–3506, Jun. 2015, doi: 10.1002/ADMA.201500604.

[116] B. Xu *et al.*, "Achieving remarkable mechanochromism and white-light emission with thermally activated delayed fluorescence through the molecular heredity principle," *Chem Sci*, vol. 7, no. 3, pp. 2201–2206, Feb. 2016, doi: 10.1039/C5SC04155D.

[117] C. E. Shuck, K. Ventura-Martinez, A. Goad, S. Uzun, M. Shekhirev, and Y. Gogotsi, "Safe Synthesis of MAX and MXene: Guidelines to Reduce Risk During Synthesis," *ACS Chemical Health & Safety*, vol. 28, no. 5, pp. 326–338, Sep. 2021, doi: 10.1021/ACS.CHAS.1C00051.

[118] M. Naguib *et al.*, “Two-dimensional transition metal carbides,” *ACS Nano*, vol. 6, no. 2, pp. 1322–1331, Feb. 2012, doi: 10.1021/NN204153H.